tuations in initial $^{234}U/^{238}U$ ratio is probably thousands of years), we are unable to take advantage of replicate analyses to diminish the ^{234}U age uncertainties. Nonetheless, ^{234}U ages are more precise than the corresponding ^{230}Th ages for samples older than 450 ka and provide a useful check on the validity of the oldest ^{230}Th ages. The agreement between ^{234}U ages and ^{230}Th ages (Table 1) for the samples that formed >350 ka (and especially for those that formed >500 ka), independently confirms the ^{230}Th ages, and also shows that the growth rate of the vein for its first 100,000 years was similar to its long-term average growth rate.

Overall, the U-series ages form a remarkably self-consistent suite of age determinations. Because this consistency is both internal (from replicate samples) and external (from the stability of the overall age-distance trend), it seems highly unlikely that the dates have been significantly corrupted by open-system processes such as uranium gain or loss or alpha-recoil phenomena. The apparent ideality of the U-Th system in the vein material is probably the result of continuous submergence in water that showed limited secular variation of its physical and chemical properties (*2*).

REFERENCES AND NOTES

1. I. J. Winograd *et al.*, *Science* **258**, 255 (1992).
2. A. C. Riggs, in preparation.
3. J. H. Chen, R. L. Edwards, G. J. Wasserburg, *Earth Planet. Sci. Lett.* **80**, 241 (1986); R. L. Edwards, J. H. Chen, G. J. Wasserburg, *ibid.* **81**, 175 (1986).
4. Isotopic analyses were done with a VG-54E single-collector mass spectrometer using an analogue-mode Daly detector, controlled by the program ANALYST [K. R. Ludwig, *U.S. Geol. Surv. Open-File Rep. 85-141* (1985)]. U was analyzed in automatic mode with $^{235}U^+$ beams of $\sim 5 \times 10^{-14}$ A ($^{238}U/^{235}U$ ratio assumed to be 137.88); Th was typically analyzed with $^{230}Th^+$ beams of $\sim 10^{-15}$ A.
5. Internal variance is variance in isotopic ratios from within-run, MS measurement only. External variance is variance in isotopic ratios not accounted for by the internal variance.
6. Amplifier nonlinearity was calibrated by measurement of fractionation-corrected $^{235}U/^{238}U$ ratio over an ion-beam range of 5×10^{-16} to 4×10^{-13} A. A slightly nonlinear response of the Daly detector was detected, with ~0.3% less gain at 4×10^{-13} A than at 5×10^{-16} A. This (software-corrected) change in gain was approximately linear with beam size, and corrections were much less than measurement precision. A regression of $^{234}U/^{235}U$ ratio versus ion-beam intensity for hundreds of blocks of standard runs shows no resolvable residual nonlinearity. Mass fractionation during measurements was corrected by normalizing to measured $^{233}U/^{236}U$ ratios (from the 1:1 ^{233}U:^{236}U spike). No fractionation correction was applied to $^{230}Th/^{229}Th$ or $^{232}Th/^{229}Th$ ratios, because the average effect on $^{230}Th/^{229}Th$ was canceled out by the similarly uncorrected spike calibrations, and fractionation corrections on the $^{230}Th/^{232}Th$ ratio were unimportant. Each Re filament was doped with graphite before use, heated to running temperature in the mass spectrometer, and examined for mass-spectral purity. Isobaric interferences were absent during data acquisition, and blank levels of ^{230}Th were close to zero (average = $-0.8 \pm 4.0 \times 10^6$ atoms). Blanks for ^{238}U were negligible (median = 1.2×10^{-11} g), although blanks for ^{232}Th were significant (median = 4.6×10^{-12} g). Tails under the small peaks from nearby large peaks were insignificant (abundance sensitivity at 1 atomic mass unit offset was 2 to 4 ppm), as were amplifier time-constant effects.
7. Uraninite standard HU-1, obtained from M. Ivanovich, yielded U-Pb isotopic ages of 620 million years ago, concordant to within 0.5% (K. R. Ludwig, unpublished data). Alpha-spectrometric measurements yielded $^{234}U/^{238}U$ activity ratios of 0.9982 ± 0.0088 and $^{230}Th/^{234}U$ activity ratios within 0.5% of unity (J. N. Rosholt, personal communication to M. Ivanovich, 1979). The Precambrian age, concordance of U/Pb isotopic ages, and alpha-spectrometric measurements all indicate that the HU-1 standard is in, or very close to, secular equilibrium for $^{230}Th/^{238}U$ and $^{234}U/^{238}U$ ratios.
8. MSWD (mean square of weighted deviates) = 0.54.
9. MSWD = 2.0.
10. For a ^{238}U half-life of 4.4683×10^9 years [A. H. Jaffey, K. R. Flynn, L. E. Glendenin, W. C. Bentley, A. M. Essling, *Phys. Rev. C* **4**, 1889 (1971)].
11. P. de Bièvre *et al.*, in *Proceedings of the International Conference on Chemical and Nuclear Data, Measurement and Applications*, M. L. Hurrell, Ed. (Institute of Civil Engineers, London, 1971), pp. 221–225. Uncertainty given at 3σ level.
12. I. J. Winograd, B. J. Szabo, T. B. Coplen, A. C. Riggs, *Science* **242**, 1275 (1988).
13. J. W. Meadows, R. J. Armani, E. L. Callis, A. M. Essling, *Phys. Rev. C* **22**, 750 (1980).
14. For all samples, systematic age errors arising from uncertainty in the ^{230}Th half-life (*13*) are smaller than those from analytical errors (because of the error-demagnification effect of normalizing to the isotopic ratios of the secular-equilibrium standard). For those samples where ^{230}Th ages are preferred over ^{234}U ages, the worst-case age error from ^{230}Th decay-constant uncertainty is 1150 years (for the 235.9-ka samples at 111 mm), compared to the analytical error for that sample of 3100 years. Errors from ^{230}Th decay-constant uncertainties for all other samples <400 ka are less; errors for 400- to 600-ka samples rise exponentially from ~0 to 10 ka. Age errors arising from uncertainty in the ^{234}U half-life (*11*) are negligible for all samples.
15. For example, a 0.2% departure in the $^{230}Th/^{238}U$ ratio of the HU-1 standard from secular equilibrium would result in systematic ^{230}Th age errors that are negligible for the samples <300 ka, and about half the analytical error for the samples with ages from 327.5 to 438 ka.

16. Supported in part by the Climate Change Program of the U.S. Geological Survey.

22 April 1992; accepted 21 August 1992

Regulation of the Amount of Starch in Plant Tissues by ADP Glucose Pyrophosphorylase

David M. Stark, Kurt P. Timmerman,* Gerard F. Barry, Jack Preiss, Ganesh M. Kishore†

Starch, a major storage metabolite in plants, positively affects the agricultural yield of a number of crops. Its biosynthetic reactions use adenosine diphosphate glucose (ADPGlc) as a substrate; ADPGlc pyrophosphorylase, the enzyme involved in ADPGlc formation, is regulated by allosteric effectors. Evidence that this plastidial enzyme catalyzes a rate-limiting reaction in starch biosynthesis was derived by expression in plants of a gene that encodes a regulatory variant of this enzyme. Allosteric regulation was demonstrated to be the major physiological mechanism that controls starch biosynthesis. Thus, plant and bacterial systems for starch and glycogen biosynthesis are similar and distinct from yeast and mammalian systems, wherein glycogen synthase has been demonstrated to be the rate-limiting regulatory step.

The α-1,4 glucans (starch and glycogen) are the main storage carbohydrates in practically all living systems (*1*). In several crops, starch is a major component of the harvest and thus directly has an impact on yield. Within the last 10 years, the demand for starch has dramatically increased for both specialized food and industrial uses (*2*), primarily as a result of the development of high fructose corn syrups and bio-ethanol. A number of specialty starches (such as amylose and waxy starch) are being increasingly recognized for their superior material and nutritional properties as well as biodegradability. Understanding the critical components of the plant starch biosynthetic machinery therefore has a major impact on agriculture and industry. We have used transgenic plants to probe the rate-limiting step in starch biosynthesis.

Starch biosynthesis occurs in the plastids of plant cells, involving ADPGlc pyrophosphorylase (E.C. 2.7.7.27), starch synthase (E.C. 2.4.1.21), and branching enzyme (E.C. 2.4.1.18) (*1*, *3*). In view of its sensitivity to allosteric effectors, ADPGlc pyrophosphorylase (ADPGPP) has been suggested to play a pivotal role in plant starch biosynthesis, as it is in the bacterial pathway for glycogen biosynthesis.

The *Escherichia coli* ADPGPP, encoded by the *glg*C gene (*4*), is a regulated ho-

D. M. Stark, K. P. Timmerman, G. F. Barry, G. M. Kishore, Monsanto Company, 700 Chesterfield Village Parkway, St. Louis, MO 63198.
J. Preiss, Department of Biochemistry, Michigan State University, East Lansing, MI 48824.

*Present address: Pioneer Hi-Bred, 7300 Northwest 62 Avenue, Johnston, IA 50131.
†To whom correspondence should be addressed.

motetrameric enzyme that is activated by fructose 1,6-bisphosphate (FbP) (5). FbP increases the catalytic activity (V_{max}), reduces the Michaelis constant (K_m) for the substrates, and decreases the sensitivity of the enzyme to the inhibitors adenosine monophosphate (AMP) and inorganic phosphate (P_i) (5, 6). A mutant *E. coli* K12 strain, 618, accumulates approximately 33% higher quantities of glycogen than its wild-type parent as a result of an alteration in the regulatory properties of ADPGPP (7). This mutant enzyme is less dependent on the activator, FbP, and is less sensitive to inhibition by the inhibitor AMP. The mutant *glgC16* gene encodes a protein with a substitution of aspartic acid for glycine at position 336 in the ADPGPP enzyme (8, 9).

Plant ADPGPPs are tetramers that contain two distinct subunits and are regulated by 3-phosphoglyceric acid (PGA) and P_i as positive and negative effectors, respectively (1). Although both large and small subunits (10–13) show homology to the *E. coli* ADPGPP enzyme, the individual subunits do not appear to be catalytically active as shown by the absence of significant enzyme activity of the maize and *Arabidopsis thaliana* starch-deficient (ADPGPP) mutants (1, 14). In view of the difficulties involved in coordinating the expression of two distinct genes, we used the *E. coli glg*C gene to probe the regulation of metabolic flux by ADPGPP. Furthermore, to minimize interference by the complex allosteric regulation of the wild-type *E. coli* gene, we used the mutant *glgC16* gene.

Because starch biosynthesis occurs in plastids, we targeted the *glgC16* gene product to plastids using a modified chloroplast transit peptide (CTP) derived from an *Arabidopsis* small subunit ribulose 1,5-bisphosphate carboxylase (*rbc*S) gene (15, 16). Uptake and processing of the fusion protein (CTP-ADPGPP) by chloroplasts was confirmed by incubation of radiolabeled fusion protein with chloroplast preparations from lettuce leaves (17) (Fig. 1).

Because the *E. coli* enzyme is a homotetramer and its interaction with plant ADPGPP subunits is not known, we determined if the CTP-*glgC16* gene product is enzymatically active in plant cells using a transient expression system (18). The chimeric CTP-*glgC16* gene was introduced by electroporation into tobacco protoplasts under control of the cauliflower mosaic virus (CaMV)–enhanced 35S (e35S) promoter (19) and the polyadenylation signal derived from nopaline synthase (NOS) encoded by the nopaline synthase gene (*Nos*) (20) (Fig. 2); the activity of the gene product was assayed. Extracts of protoplasts electroporated with the chimeric gene displayed P_i-resistant ADPGPP activity, whereas the controls had little or no activity under these conditions (Fig. 3). Thus, the *E. coli* mutant gene could be expressed in plant cells, and the gene product retains its enzymatic activity and phosphate insensitivity.

To produce stable transgenic plants that express the CTP-*glgC16* gene, we mated the pMON20104 plasmid containing a NOS-*NPTII* (neomycin phosphotransferase) gene as the selectable marker into *Agrobacterium tumefaciens* strain ASE and subsequently used it for the transformation of tobacco (21), tomato (22), and potato (23). Calli and shoots resulting from transformation and displaying resistance to kanamycin were analyzed for expression of the CTP-*glgC16* gene and starch content. The examination of transgenic and control tobacco calli by light microscopy revealed substantial differences in the number of starch granules (Fig. 4). Protein immunoblot and quantitative starch analyses on 12 independent transgenic and 2 control lines showed that calli that expressed the CTP-*glgC16* gene contained on average 10.7% starch (SD = 6.2, on the basis of dry weight), a significant increase ($P = 0.0017$, Welch analysis of variance (ANOVA) *t* test for unequal variance) over controls that contained 3.4% starch (SD = 0.5). One of the samples expressing the CTP-*glgC16* gene contained 26.9% starch (Fig. 5). These observations establish that the ADPGPP reaction is the rate-limiting step in starch biosynthesis in tobacco cells. Even in tomato leaves, which typically do not accumulate large amounts of starch, a cor-

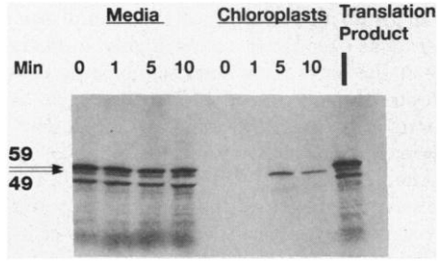

Fig. 1. Import and processing of the CTP-ADPGPP fusion protein by chloroplast preparations of lettuce (*Lactuca sativa* var. longifolia). Molecular size markers are indicated to the left in kilodaltons. The CTP-*glgC16* gene in pMON20100 was amplified by PCR with the use of an SP6 promoter primer (Promega, Madison, Wisconsin) and the primer used for introducing the Sac I site at the 3′ end of the *glgC16* gene. The PCR product was purified by agarose gel electrophoresis and binding to a DEAE membrane. The purified DNA was incubated with SP6 RNA polymerase (Promega). The resulting RNA was translated in rabbit reticulocyte lysate (Promega) containing [^{35}S]methionine, the 19–amino acid mixture, RNA, and RNasin (Promega). SDS–gel electrophoresis of the resulting translation product demonstrated that at least two major radiolabeled proteins were produced. The slowest migrating band had a molecular size expected for the CTP-ADPGPP fusion protein (59 kD). The additional smaller bands arise from internal initiation of translation. The radiolabeled translation product was incubated for 1 to 10 min with intact chloroplast preparations from lettuce, obtained as described (17). The medium and chloroplasts in the incubation mix were separated by silicone-oil gradient centrifugation, and the chloroplast fraction was treated with trypsin. Both fractions were then treated with SDS buffer for electrophoresis. SDS–polyacrylamide gel electrophoresis was conducted with the use of a 3 to 17% polyacrylamide gradient. The gel was fixed, soaked in EN3HANCE (NEN, Boston, Massachusetts), dried, and imaged by autoradiography with the use of an intensifying screen and overnight exposure at −70°C. The 1-, 5-, and 10-min radiolabel bands in the chloroplast fractions were trypsin-resistant, which indicates that they were present within the organelle.

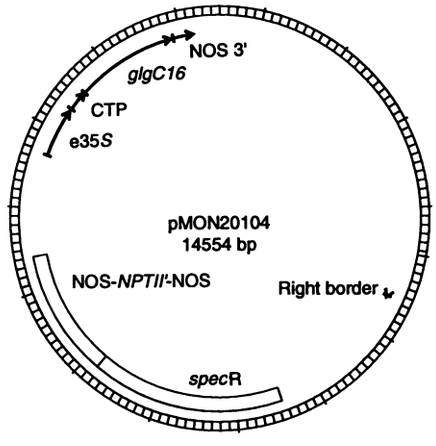

Fig. 2. A schematic representation of the chimeric 35*S* promoter-CTP-*glgC16-Nos* gene and the transferred DNA vector (pMON20104). To express the CTP-*glgC16* gene in both transient as well as stably transformed plant cells, we created a Bgl II site 7 bp upstream of the ATG translation initiation codon of the CTP in pMON20100. Xba I and Sac I sites were introduced after the termination codon in *glgC16* in the same construct. These mutations were introduced by PCR mutagenesis with the use of appropriate primers. The PCR product was digested with Bgl II and Sac I. The vector, pMON999, which contains the e35*S* promoter and the *Nos* 3′ polyadenylate signal, was digested with Bgl II and Sac I. The product of the PCR reaction was ligated with the vector, and the result was transformed into *E. coli* MM294. The resulting plasmid, pMON20102, contained a 2.5-kb Not I fragment that consisted of the e35*S* promoter, CTP-*glgC16*, and the *Nos* terminator. The Not I cassette was transferred to the plant transformation vector pMON530 (34), and the resulting plasmid was designated pMON20104. The spectinomycin resistance gene is indicated by *spec*R.

relation was observed between the presence of the bacterial ADPGPP and starch content (Fig. 4C).

Our attempts to regenerate plants that expressed the CTP-*glgC16* gene under the control of the e35S promoter resulted in poor recovery of plants expressing the gene. Our interpretation of these observations is that constitutive expression of the CTP-*glgC16* gene, as directed by the CaMV 35S promoter, is detrimental to plant growth and development. Excess starch accumulation in the leaves may reduce sucrose availability for export and thus restrict the amount of carbon available to the actively growing portions of the plant. This decrease in available sucrose also may affect the turgor of a number of different plant cells and tissues. In accord with these observations, a transgenic potato plant that expressed the e35S/CTP–*glgC16*/*Nos* gene was recovered that could be maintained on a sucrose-containing medium but could not survive in soil when sucrose was not provided in the growth medium.

To overcome the detrimental effects of constitutive ADPGPP activity, we introduced the CTP-*glgC16* gene into potato plants under the control of a tuber-specific patatin promoter (*24*). We recovered numerous transgenic plants (*25*) with a transformation efficiency typical for potato, and plants that expressed this gene had a normal phenotype. Specific gravity measurements, which indicate tuber density and thus starch content (*26*), show that tubers expressing the patatin-CTP-*glgC16* gene contain, on average, 35% more starch than control tubers (Fig. 6 and Table 1). Some transgenic potato lines produced tubers with nearly 60% more starch than controls. This range of specific gravity values in control and transgenic lines is typical of potato and has been documented (*27*). Chemical determination of starch content from a sampling of tubers confirmed that specific gravity was a valid reflection of starch content (Table 2). Therefore, tissue-specific expression of the CTP-*glgC16* gene with the use of a patatin promoter results in significant increases in starch content without adverse effects on plant growth or development. Recently, similar results were obtained in a small-scale field trial (*25*), which indicates that ADPGPP activity is rate-limiting for tuber starch biosynthesis even under conditions of potato cultivation.

Whereas the presence of the CTP-*glgC16* gene product was absolutely required for increased starch production, the extent of starch content increase was not absolutely correlated with the level of expression of *E. coli* ADPGPP enzyme protein in all the tubers (Table 3). This suggests that expression of small amounts of the CTP-*glgC16* gene may be sufficient to overcome the limitation of ADPGlc availability for starch biosynthesis and to create a new rate-limiting step. Alternatively, substrate availability (glucose 1-phosphate) for the ADPGPP reaction may itself become rate limiting. Which of these mechanisms is operative under physiological conditions can now be investigated using these transgenic potato plants.

In vitro studies that use *Commelina* guard-cell chloroplast extracts have shown that the activity of starch synthase is only one-twentieth that of ADPGPP and the branching enzymes (*1*, *28*). These results imply that starch synthase is the rate-limiting reaction in starch biosynthesis. In view of our finding that enhanced ADPGPP activity increases the starch content of plant cells, we reasoned that allosteric regulation may down-regulate ADPGPP activity under in vivo conditions. To evaluate the importance of allosteric regulation in the control of ADPGPP activity and starch content, we fused the wild-type *E. coli glgC*

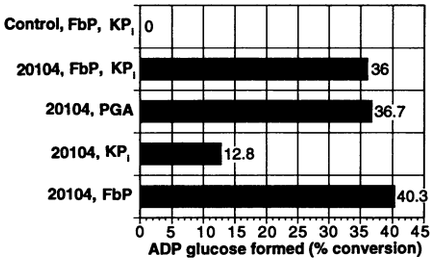

Fig. 3. ADPGPP activity in protoplasts. Plasmid pMON20104 was subject to electroporation into tobacco TXD protoplasts (*18*). Plasmid pMON999 was used as the control. The protoplasts were separated from the medium by centrifugation and washed with 100 mM tris EDTA buffer (pH 7.5) that contained 35 mM KCl and 20% glycerol. The pellet was suspended in the extraction buffer [200 μl of washing buffer that contained 5 mM dithiothreitol (DTT), 1 mM benzamidine, and 5 mM sodium ascorbate per 50 μl of protoplast volume] and sonicated for 2 min. The resulting suspension was centrifuged to remove the insoluble pellet, and the supernatant was desalted on a Sephadex G-50 (Sigma) spin column equilibrated with extraction buffer. The enzyme assay mix contained in 100 μl: 10 μmol Hepes (pH 7.7), 50 μg of bovine serum albumin, 0.05 μmol ^{14}C-glucose 1-phosphate, 0.15 μmol of adenosine 5′-triphosphate, 0.5 μmol of $MgCl_2$, 0.1 μg of crystalline yeast inorganic pyrophosphatase, 1 mM ammonium molybdate, and water. Fructose 1,6-bisphosphate (FbP) (2.5 mM) or 3-phosphoglycerate (20 mM) was added as indicated to activate the *E. coli* or plant ADPGPP enzymes, respectively. To further distinguish endogenous ADPGPP activity from that of the *E. coli* ADPGPP mutant, we added 10 mM inorganic phosphate (KP_i), which completely inhibits the plant enzyme but does not affect the *E. coli* enzyme. The enzymatic reaction was carried out at 37°C for 10 min and stopped by incubation in a boiling water bath for 1 min. After centrifugation to remove the denatured protein, 40 μl of supernatant was loaded on a SynChropak AX100 (SynChrom, Lafayette, Indiana) column (250 × 4.6 mm) and eluted with 65 mM KP_i (pH 5.5) at a flow rate of 1 ml per minute. The radioactivity of the eluate was followed with the use of a Radiomatic (Radiomatic Instruments, Tampa, Florida) detector. Glucose 1-phosphate eluted at 8.3 min, and ADPGlc eluted at 14 min under these conditions. The radioactivity in the ADPGlc peak was a measure of the ADPGPP activity of the sample. Protein content of the extract was measured by the Bradford method (*35*) with the use of the Bio-Rad reagent.

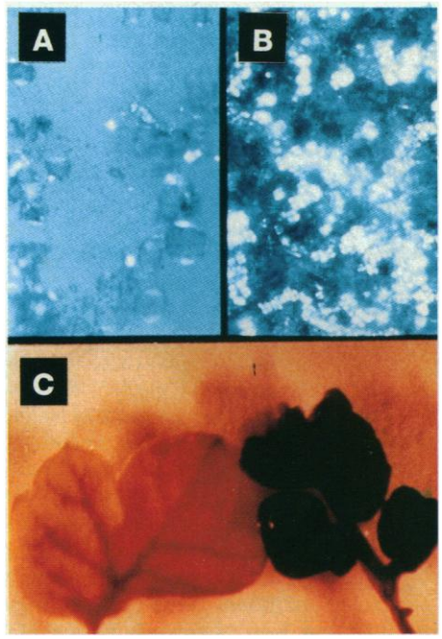

Fig. 4. (**A**) Polarizing photomicrograph of a cross section of tobacco callus tissue transformed with vector control DNA. Leaf disks of tobacco were transformed (*21*) with *Agrobacterium* strain ASE containing the pMON530 vector. After 2 to 3 weeks, calli formed, and the individual clumps were separated from the leaf disks. The starch granules appear as white, birefringent structures. (**B**) Polarizing photomicrograph of a cross section of tobacco callus tissue transformed as in (A) with pMON20104. (**C**) Iodine-stained transgenic tomato shoot expressing the CTP-*glgC16* gene (right) and a tomato shoot not containing the CTP-*glgC16* gene. pMON16927 was constructed by ligation of the CTP-*glgC16* chimeric gene from pMON20102 as a Bgl II–Sac I fragment into the binary vector pMON977 (*34*). Cotyledons of *Lycopersicon esculentum* cv. UC82B were transformed (*22*) by *Agrobacterium* strain ABI containing pMON977 for control and pMON16927 for CTP-*glgC16* expression. After 2 to 3 weeks, shoots were cleanly excised from the callus, decolored in 70% ethanol for 1 hour, and stained in a solution of 0.2% I_2 and 0.4% KI.

gene with the CTP and expressed it in potato tubers and in tomato leaves using the patatin and *Arabidopsis rbc*S promoters, respectively. Unlike the GlgC16 enzyme, wild-type GlgC is fully subject to allosteric regulation (*4*). However, the primary effector molecules differ between the plant and bacterial enzymes. Thus, depending on the relative concentrations of these effectors in vivo, expression of the CTP-*glg*C gene may also result in increased ADPGPP activity and starch content in a plant cell environment. Expression, enzyme activity, and plastid targeting from the cloned *glg*C gene were confirmed before plant transformation (*29*). A large number of tomato plants transformed with the *rbc*S-CTP-*glg*C gene were obtained and were phenotypically normal. Analyses of leaf tissue showed high levels (0.1% of total protein) of expression of the CTP-*glg*C gene but only a slight effect on starch content (Table 4). The increase in average starch content of 11.2% was not significant (*t* test, $P = 0.3111$). By contrast, recovery of plants with leaf expression of CTP-*glg*C16 was very poor, similar to the lethal effect seen with the e35S promoter.

In potato tubers, expression of CTP-*glg*C did not result in a noticeable increase in starch content (Table 5), even though expression levels were equivalent to those in tubers that expressed CTP-*glg*C16. We conclude that CTP-*glg*C expression may lead to a slight, but not significant, amount of starch increase in plant tissues. The kinetic characteristics of the GlgC and GlgC16 enzymes have been reported (*7–9*) and differ primarily in allosteric regulation. The V_{max} of each enzyme is the same under fully activated conditions. On the basis of these features, our work represents further evidence that ADPGPP activity is rate limiting in starch biosynthesis and that it is the regulatory properties of ADPGPP, not the amount of enzyme protein, that make it rate limiting.

We investigated the effect of cytosol-targeted expression of GlgC16 by localizing the *glg*C16 gene product within the cytosol of potato tuber cells. Amounts of *glg*C16 gene product were slightly smaller than amounts of the CTP-*glg*C16 gene product (0.02 to 0.05% versus 0.02 to 0.1% of total tuber protein) but were within the range of expression seen in high-starch CTP-*glg*C16 tubers. Cytosolic lo-

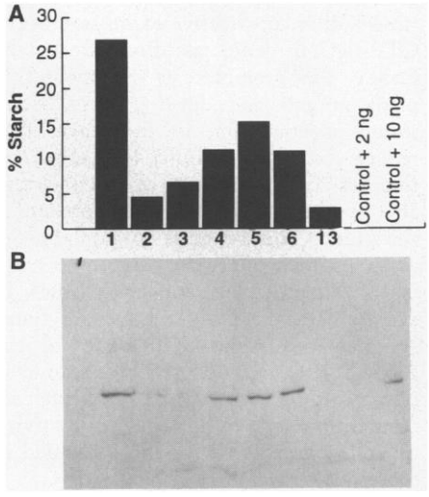

Fig. 5. Starch content (**A**) and protein immunoblot analysis (**B**) of tobacco calli. Samples 1 through 6 express the *glgC16* gene, sample 13 is a control lacking the *glgC16* gene, and the last two lanes are sample 13 with either 2 or 10 ng of GlgC16 protein purified from *E. coli*. Starch levels in transformed tobacco calli were quantitated with the method of Lin *et al.* (*14*). Differences are significant with the use of the Welch ANOVA *t* test for unequal variance ($P = 0.0017$). For protein immunoblot analysis, a portion of the dried, homogeneous callus from each of the experimental and control samples was suspended in 200 μl of extraction buffer [100 mM tris-Cl (pH 7.1), 1 mM EDTA, 10% glycerol, 5 mM DTT, and 1 mM benzamidine]. We ground each sample to extract the protein and centrifuged the samples to remove insoluble debris. The protein concentration of the supernatant was estimated with the use of Bradford reagent, and 25 μg of protein from each sample was loaded on SDS–polyacrylamide gels, with a 7 to 17% gradient. After electrophoresis, the gels were blotted onto nitrocellulose, and the *E. coli* ADPGPP was visualized with the use of rabbit anti-ADPGPP as the primary antibody and goat anti-rabbit serum conjugated to alkaline phosphatase as the secondary antibody. The reaction of alkaline phosphatase with nitro blue tetrazolium and 5-bromo-4-chloro-3-indoyl phosphate was used for color development.

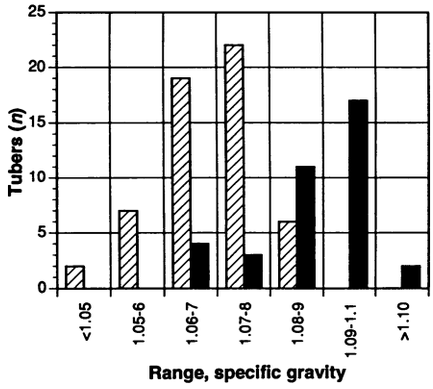

Fig. 6. Specific gravity of potato tubers expressing CTP-*glgC16*. We generated pMON20113 by replacing the CaMV 35*S* promoter in pMON999 with a 1-kb Hind III–Bam HI fragment that contained a portion of a class I patatin promoter (*24*). The *glgC16* gene from pMON20104, including the chloroplast transit peptide derived from the ribulose 1,5-biphosphate carboxylase small subunit 1A gene of *Arabidopsis*, was then added as a Bgl II–Sac I fragment, and the entire patatin promoter–CTP-*glgC16*-NOS 3′ end cassette was cloned as a Not I fragment to the binary vector pMON886 (*34*). Potato var. Russet Burbank was transformed with *Agrobacterium* strain ASE containing the pMON20113 vector (*23*). Control transformations were performed with the use of the vector pMON886. Tubers from regenerated plants were screened for the expression of GlgC16 by protein immunoblot (Fig. 5). Fifteen CTP-*glgC16*–positive and 21 control plants were screened, and specific gravity was determined for two to three tubers per plant. Solid and hatched bars represent the numbers of tubers for those expressing *E. coli* ADPGPP and for control tubers, respectively, that fell within the indicated range of values. Controls consisted of a combination of tubers transformed to contain only the vector DNA and tubers from the *glgC16* transformation event that do not express *E. coli* ADPGPP.

Table 1. Average specific gravity and starch content is increased in tubers that express the CTP-*glgC16* gene. The number of independent plant lines tested is indicated, with two or three tubers per plant weighed. Specific gravity was determined by the weight-in-air–weight-in-water method (*26*). Sample standard deviations (SD) of the specific gravity measurements are indicated. Percent starch was calculated from the average specific gravity as described (*26*). Controls consist of a combination of Russet Burbank tubers transformed to contain only the vector DNA and tubers from the *glgC16* transformation event that do not express *E. coli* ADPGPP.

Tuber type	Plant lines	Average specific gravity	SD	Average % starch
CTP-GlgC16	15	1.088	0.012	15.4
Control	21	1.068	0.010	11.4

Table 2. Average values for percent starch determined experimentally by enzymatic degradation (*14*) compared to starch content calculated from specific gravity measurements. Sample standard deviations are in parentheses. Differences between the methods for starch determination are not significant. However, differences between CTP-GlgC16+ and controls, calculated by specific gravity or enzymatic methods, are significant by the *t* test ($P < 0.0001$). Tuber types are as in Table 1.

Tuber type	Sample size	Average % starch specific gravity	Average % starch enzymatic
CTP-GlgC16	11	16.3 (1.47)	16.0 (2.00)
Control	11	11.9 (1.56)	12.3 (1.15)

Table 3. Comparison of expression levels of CTP-*glgC16* and their effects on starch content. CTP-*glgC16* levels were estimated from protein immunoblot analysis by comparison to known standards. Starch content was determined by the enzymatic degradation method. One tuber [Russet Burbank (R.B.)] from each line was used for both analyses. Control starch levels represent the average value for 12 tubers.

Tuber type	Range (ng of CTP-*glgC16* per 50 μg of protein)	Range (% starch, fresh weight)
R.B. control	0	5.4 to 14.4
R.B. + high GlgC16	26 to 50	14.4 to 19.2
R.B. + medium GlgC16	10 to 25	11.8 to 19.1
R.B. + low GlgC16	0.5 to 10	8.8 to 17.4

Table 4. Starch content of tomato leaves expressing CTP-*glgC*. The wild-type CTP-*glgC* gene was engineered for expression in plants essentially as described for the CTP-*glgC16* gene (*16*) (Figs. 2 and 6). The CTP-*glgC* gene was added to a derivative of the binary vector pMON977 (*34*), which contains the *Arabidopsis* promoter from the *rbc*S gene (*15*) in place of e35*S*, resulting in the plasmid pMON16938. *Lycopersicon esculentum* cv. UC82B (*L.e.*) was transformed (*22*) with *Agrobacterium* strain ABI containing the vector pMON16938. The subsequent R1 generation was screened for the expression of CTP-GlgC in leaves by protein immunoblot. Standard deviations (SD) are indicated. Starch content was determined (*14*) in leaf tissue taken from plants at the end of the light cycle. Values are not significantly different (*t* test, $P = 0.3111$).

Leaf type	Plants (*n*)	Average % starch (fresh weight)	SD
L.e. + CTP-GlgC	14	9.3	1.8
L.e. control	10	8.4	2.7

calization of the *glgC16* gene product, however, did not result in a significant effect on starch content (Table 6).

Recently, there has been controversy concerning the subcellular location of ADPGlc synthesis in plant cells. Because under in vitro conditions cytosol-localized sucrose synthase uses ADP as a substrate and plastids import ADPGlc, it has been suggested that sucrose synthase serves as a source of ADPGlc for starch biosynthesis in plant cells and tissues (*30*). However, in view of our demonstration that only the expression of CTP-*glgC16*, not *glgC16*, results in an increased starch content, it is unlikely that this mechanism contributes significantly to starch biosynthesis. Further evidence in support of the plastidial ADPGPP pathway comes from recent work that shows that reduction of the plant ADPGPP enzyme level by means of antisense RNA results in decreased starch formation (*31*).

Because potato tubers that express the CTP-*glgC16* gene contain more starch, it would be interesting to determine if this is a result of the ability of the potato plant to provide additional photosynthate to the tuber or a result of a reduction in water content of the tuber due to rapid conversion of the osmotically active sugars to starch. Evidence exists that plants contain unused photosynthetic capacity that could become available should the demand be present (*32*). This is supported by numerous reports that show that increased carbon demand results in increased assimilation in and output from the leaves (*33*).

ADPGPP has been suggested to influence the ability of tubers to import carbon and convert it into starch—that is, the rate of starch accumulation regulates the rate of carbon import (*1*); this hypothesis is now supported by our study. The transgenic potato plants described here will allow the testing of models that suggest that photosynthetic carbon assimilation is not limiting to yield. It is interesting that a single enzymatic step regulates the end-product levels to such a dramatic extent in a complex multicellular organism. With a similar approach, it should be possible for researchers to manipulate the amounts of a number of key metabolites such as lipids, amino acids, and carbohydrates by affecting or altering a major regulatory step in the biosynthesis of relevant metabolites.

Table 5. Starch content of potato tubers that express CTP-*glgC*. The CTP-*glgC* gene was ligated into a derivative of the binary vector pMON977 containing the patatin promoter in place of e35*S*, resulting in the plasmid pMON16950. Potato var. Russet Burbank was transformed with *Agrobacterium* strain ABI containing the pMON16950 vector (*23*). Analysis of tubers from regenerated plants was as described (Table 1). Starch content was determined as in Table 1.

Tuber type	Plant lines	Average specific gravity	SD	Average % starch
R.B. + CTP-GlgC	6	1.076	0.005	13.1
R.B. control	17	1.077	0.010	13.2

Table 6. Specific gravity and starch content of potato tubers that express GlgC16 in the cytosol. A cytosolic version of the *glgC16* gene was created by ligation of the coding region from pMON20100 as a Nco I and Sac I fragment into a version of pBluescript kS+ (Stratagene, La Jolla, California) engineered to contain Bgl II and Nco I sites in the polylinker. The coding region was then ligated as a Bgl II and Sac I fragment into the binary vector pMON16952, which contains the class I patatin promoter, resulting in the plasmid pMON16971. Potato var. Russet Burbank was transformed with *Agrobacterium* strain ABI containing the pMON16971 vector (*23*). Tubers formed from regenerated plants were analyzed as described (Table 1).

Tuber type	Plant lines	Average specific gravity	SD	Average % starch
GlgC16+	26	1.073	0.010	12.4
Controls	22	1.073	0.008	12.4

REFERENCES AND NOTES

1. J. Preiss, in *The Biochemistry of Plants*, J. Preiss, Ed. (Academic Press, Orlando, FL, 1988), pp. 184–249; in *Oxford Survey of Plant Molecular and Cellular Biology*, B. J. Miflin, Ed. (Oxford Univ. Press, Oxford, 1991), vol. 7, pp. 59–114.
2. F. R. Katz, in *Biotechnology and Food Ingredients*, I. Goldberg and R. Williams, Eds. (Van Nostrand Reinhold, New York, 1991), pp. 315–326.
3. E. Beck and P. Zeigler, *Annu. Rev. Plant Physiol. Plant Mol. Biol.* **40**, 95 (1989).
4. T. W. Okita, R. L. Rodriguez, J. Preiss, *J. Biol. Chem.* **256**, 6944 (1981).
5. J. Preiss, L. Shen, E. Greenberg, N. Genter, *Biochemistry* **5**, 1833 (1966).
6. N. Gentner and J. Preiss, *J. Biol. Chem.* **243**, 5882 (1968); J. Preiss and T. Romeo, *Adv. Bact. Physiol.* **30**, 184 (1989).
7. J. Cattaneo, M. Damotte, N. Sigal, F. Sanchez-Medina, J. Puig, *Biochem. Biophys. Res. Commun.* **34**, 694 (1969); N. Creuzet-Sigal, M. Latil-Damotte, J. Puig, in *Biochemistry of the Glycosidic Linkage*, R. Piras and H. G. Pontis, Eds. (Academic Press, New York, 1972), vol. 2, pp. 647–680.
8. P. Leung *et al.*, *J. Bacteriol.* **167**, 82 (1986).
9. Y. M. Lee, A. Kumar, J. Preiss, *Nucleic Acids Res.* **15**, 10603 (1987); J. Preiss and M. A. Hill, unpublished results.
10. J. M. Anderson *et al.*, *J. Biol. Chem.* **264**, 12238 (1989).
11. M. R. Olive, R. J. Ellis, W. W. Schuch, *Plant Mol. Biol.* **12**, 525 (1989).
12. M. R. Bhave, S. Lawrence, C. Barton, L. C. Hannah, *Plant Cell* **2**, 581 (1990).
13. B. T. Muller, J. Koßmann, L. C. Hannah, L. Willmitzer, U. Sonnewald, *Mol. Gen. Genet.* **224**, 136 (1990); P. A. Nakata *et al.*, *Plant Mol. Biol.* **17**, 1089 (1991).
14. T. P. Lin, T. Caspar, C. Somerville, J. Preiss, *Plant Physiol.* **86**, 1131 (1988).
15. M. P. Timko *et al.*, *Nature* **318**, 579 (1985).
16. The *Arabidopsis* CTP was generated with the use of the chloroplast-targeting and mature NH_2-terminal coding regions of the ribulose carbox-

ylase 1A gene (*rbc*S 1A) (*15*). The CTP was modified by addition of the first 23 amino acids (MQVWPPIGKKKFETLSYLPDLTDS) because the efficiency of protein import is increased by addition of the sequences from the mature region of this protein. Abbreviations for the amino acid residues are: A, Ala; C, Cys; D, Asp; E, Glu; F, Phe; G, Gly; H, His; I, Ile; K, Lys; L, Leu; M, Met; N, Asn; P, Pro; Q, Gln; R, Arg; S, Ser; T, Thr; V, Val; W, Trp; and Y, Tyr. To facilitate removal of the remaining *rbc*S sequences from the ADPGPP protein, we added a second protease cleavage site (GGRVNCMQA) between these 23 amino acids of *rbc*S and the NH_2-terminal Met of *E. coli* ADPGPP. The *glgC16* gene was obtained as a Hinc II fragment from plasmid pLP226 (*8*) and cloned into the pUC8 vector at the Hinc II site. To fuse the modified transit peptide coding region to the translation initiation site of the *glgC16* gene, we introduced an Nco I site at the initiating methionine of the *glgC16* gene. Also, to remove 3′ nucleotide sequences, we added a Sac I site downstream of the termination codon of the *glgC16* gene. Both Nco I and Sac I sites were introduced by polymerase chain reaction (PCR) mutagenesis. The modified *Arabidopsis* CTP plus the *glgC16* gene were cloned into pGEM3zf+ (Promega, Madison, WI), digested with Hind III and Sac I, by ligating the *Arabidopsis* CTP as a Hind III–Nco I fragment and *glgC16* as an Nco I–Sac I fragment. The resulting plasmid (pMON20100) consisted of pGEM3zf+, the modified *Arabidopsis* CTP, and the *glgC16* gene. The CTP-*glgC16* gene in the plasmid was in an orientation suitable for transcription by the SP6 promoter resident in the pGEM3zf+ plasmid.

17. G. della-Cioppa *et al.*, *Biotechnology* **5**, 579 (1987).
18. J. Callis, M. Fromm, V. Walbot, *Nucleic Acids Res.* **15**, 5823 (1987).
19. R. Kay, A. Chan, M. Daly, J. McPherson, *Science* **236**, 1299 (1987).
20. M. Bevan, *Nucleic Acids Res.* **12**, 8711 (1984).
21. R. B. Horsch *et al.*, *Science* **223**, 496 (1984).
22. S. McCormick *et al.*, *Plant Cell Rep.* **5**, 80 (1986).
23. C. A. Newell *et al.*, *ibid.* **10**, 30 (1991).
24. M. Bevan *et al.*, *Nucleic Acids Res.* **14**, 4625 (1986).
25. D. M. Stark, G. F. Barry, Y. M. Muskopf, K. P. Timmerman, G. M. Kishore, paper presented at the Third International Congress of Plant Molecular Biology, Tucson, AZ, 6–11 October 1991, abstract 714.
26. C. von Scheele, *Landwirtsch. Vers. Stn.* **127**, 67 (1937).
27. G. E. Kleinkopf, D. T. Westermann, M. J. Wille, G. D. Kleinschmidt, *Am. Potato J.* **64**, 579 (1987).
28. N. L. Robinson and J. Preiss, *Plant Physiol.* **85**, 360 (1987).
29. D. M. Stark, K. P. Timmerman, G. F. Barry, J. Preiss, G. M. Kishore, data not shown.
30. J. Pozueta-Romero, M. Frehner, A. M. Viale, T. Akazawa, *Proc. Natl. Acad. Sci. U.S.A.* **88**, 5769 (1991).
31. B. Muller-Rober, U. Sonnewald, L. Willmitzer, *EMBO J.* **11**, 1229 (1992).
32. R. B. Dwelle, *Am. Potato J.* **67**, 829 (1990).
33. W. S. Cranshaw and E. B. Radcliffe, *J. Econ. Entomol.* **73**, 131 (1980); R. B. Dwelle, in *Potato Physiology*, P. Li, Ed. (Academic Press, Orlando, FL, 1985), pp. 35–58; E. E. Ewing, K. P. Sandlan, A. G. Nicholson, paper presented at the 11th Triennial Conference of the European Association for Potato Research, Edinburgh, Scotland, 1990; J. Moorby, *Symp. Soc. Exp. Biol.* **31**, 425 (1977).
34. S. G. Rogers, H. J. Klee, R. B. Horsch, R. T. Fraley, in *Methods in Enzymology*, R. Wu and L. Grossman, Eds. (Academic Press, San Diego, 1987), pp. 253–277.
35 M. Bradford, *Anal. Biochem.* **72**, 248 (1976).

36. We thank N. Mathis, Y. Muskopf, J. Heinz, and J. Layton for plant transformation; J. Hart, B. LaValle, B. Schuler, T. Coombe, M. Pratt, and B. Coombs for maintenance of plants; M. Hayford for pMON999; M. Bevan for the patatin promoter; C. Hironaka for the CTP; M. Hinchee for assistance in light microscopy; and R. T. Fraley for support.

29 April 1992; accepted 31 July 1992

Intercellular Propagation of Calcium Waves Mediated by Inositol Trisphosphate

Scott Boitano, Ellen R. Dirksen, Michael J. Sanderson*

Two types of calcium (Ca^{2+}) signaling—propagating intercellular Ca^{2+} waves of increasing intracellular Ca^{2+} concentration ($[Ca^{2+}]_i$) and nonpropagating oscillations in $[Ca^{2+}]_i$—co-exist in a variety of cell types. To investigate this difference in Ca^{2+} signaling, airway epithelial cells were loaded with heparin, an inositol 1,4,5-trisphosphate (IP_3) receptor antagonist, by pulsed, high-frequency electroporation. Heparin inhibited propagation of intercellular Ca^{2+} waves but not oscillations of $[Ca^{2+}]_i$. In heparin-free cells, Ca^{2+} waves propagated through cells displaying $[Ca^{2+}]_i$ oscillations. Depletion of intracellular Ca^{2+} pools with the Ca^{2+}-pump inhibitor thapsigargin also inhibited the propagation of Ca^{2+} waves. These studies demonstrate that the release of Ca^{2+} by IP_3 is necessary for the propagation of intercellular Ca^{2+} waves and suggest that IP_3 moves through gap junctions to communicate intercellular Ca^{2+} waves.

Intercellular communication is essential for the function of multicellular systems, but the nature of the signal or signals that pass between cells through gap junctions is not fully established. Both Ca^{2+} and IP_3 have been proposed as intercellular messengers (*1–3*). Nonexcitable cells often respond to agonists by increasing their $[Ca^{2+}]_i$ in an oscillatory manner (*4*), but these oscillations in $[Ca^{2+}]_i$ occur independently of $[Ca^{2+}]_i$ changes in adjacent cells (*3*). In contrast to Ca^{2+} oscillations, a propagating intercellular wave of increased $[Ca^{2+}]_i$ (a Ca^{2+} wave) can be initiated by mechanical stimulation of a single cell in cultures of airway epithelial (*2*), rat brain glial (*3, 5, 6*), or bovine aortic endothelial (*7*) cells or by treatment of astrocytes with glutamate (*8*). In airway epithelial cells Ca^{2+} waves are blocked by the gap junction inhibitor Ca^{2+} halothane (*2*), and in C6 glioma cells only cells transfected with and expressing the gene for the gap junction protein connexin43 propagate Ca^{2+} waves (*6*). These results indicate that Ca^{2+} waves are propagated through gap junctions (*1–3, 5–8*). A role for IP_3 in the communication of Ca^{2+} waves has been proposed because Ca^{2+} waves are propagated in the absence of extracellular Ca^{2+} (*2, 3, 7*), are propagated when Ca^{2+}-induced Ca^{2+} release is inhibited (*5*), and can be initiated by microinjection of IP_3 (*2*). If IP_3 acts as the intercellular messenger for propagation of Ca^{2+} waves, intracellular heparin, an antagonist of the IP_3 receptor (*9*), should block or attenuate the Ca^{2+} wave (*9*).

Traditional loading techniques, such as microinjection, are not well suited for loading the large numbers of cells required for investigation of this multicellular response. Therefore, we used pulsed high-frequency electroporation (PHFE) (*10, 11*) to load cultured cells with heparin (Fig. 1). Because heparin cannot be detected by fluorescence microscopy, cells were simultaneously loaded with fluorescent Texas red–conjugated dextran (TRD) to identify cells that incorporated heparin (Fig. 1) (*11, 12*). PHFE has a major advantage over current-discharge electroporation in that most cells survive (*10*). After PHFE, and loading cells with fura-2 by incubation in fura-2-pentaacetoxymethyl ester (fura-2-AM) (*12*), more than 90% of the heparin-loaded cells retained fura-2 and heparin-loaded ciliated cells continued to display ciliary activity. These results demonstrate the potential of PHFE for loading cells with molecules that are impermeable to the cell membrane because of their large molecular size or ionic charge.

In an area where all cells were loaded with heparin, mechanical stimulation of a single cell increased $[Ca^{2+}]_i$ in the stimulated cell but did not initiate propagation of a Ca^{2+} wave through multiple adjacent cells, even though the increase in $[Ca^{2+}]_i$ of the stimulated cell ranged from 300 nM to >1 μM (Fig. 2A). In a few of these experiments in the heparin-loaded area, $[Ca^{2+}]_i$ increased in single cells directly adjoining the stimulated cell, but an increase of $[Ca^{2+}]_i$ in more distal cells was not observed. The increase in $[Ca^{2+}]_i$ of the stimulated, heparin-loaded cells and our reports that the $[Ca^{2+}]_i$ of a mechanically

Department of Anatomy and Cell Biology, UCLA School of Medicine, Los Angeles, CA 90024.

*To whom correspondence should be addressed.